Article

A Molecular Motor, KIF13A, Controls Anxiety by Transporting the Serotonin Type 1A Receptor

Ruyun Zhou,[1,3] Shinsuke Niwa,[1,3] Laurent Guillaud,[1] Ying Tong,[1] and Nobutaka Hirokawa[1,2,*]
[1]Department of Cell Biology, Graduate School of Medicine, University of Tokyo, Tokyo 113-0033, Japan
[2]Center of Excellence in Genome Medicine Research, King Abdulaziz University, Jeddah 21589, Saudi Arabia
[3]These authors equally contributed to this work
*Correspondence: hirokawa@m.u-tokyo.ac.jp
http://dx.doi.org/10.1016/j.celrep.2013.01.014

SUMMARY

Molecular motors are fundamental to neuronal morphogenesis and function. However, the extent to which molecular motors are involved in higher brain functions remains largely unknown. In this study, we show that mice deficient in the kinesin family motor protein KIF13A ($Kif13a^{-/-}$ mice) exhibit elevated anxiety-related behavioral phenotypes, probably because of a reduction in $5HT_{1A}$ receptor ($5HT_{1A}R$) transport. The cell-surface expression level of the $5HT_{1A}R$ was reduced in KIF13A-knockdown neuroblastoma cells and $Kif13a^{-/-}$ hippocampal neurons. Biochemical analysis showed that the forkhead-associated (FHA) domain of KIF13A and an intracellular loop of the $5HT_{1A}R$ are the interface between the motor and cargo vesicles. A minimotor consisting of the motor and FHA domains is able to transport $5HT_{1A}R$-carrying organelles in in vitro reconstitution assays. Collectively, our results suggest a role for this molecular motor in anxiety control.

INTRODUCTION

Neurotransmitter receptors are membrane proteins that are essential for neurons to communicate through chemical signals (Nicholls, 2001; Snyder, 2009). Because neurotransmitter receptors are fundamental for brain function and animal behavior, their dysfunction is thought to underlie many psychiatric disorders (Nicholls, 2001). Genetic alteration of neurotransmitter receptors has been reported to induce abnormal behavior in mice (Aiba et al., 1994; Li et al., 1994; Parks et al., 1998; Ramboz et al., 1998; Tsien et al., 1996). Serotonin (5-hydroxytryptamine [5-HT]) receptors are one class of neurotransmitter receptor. This class is known to be involved in various neurological processes, such as aggression, anxiety, and mood. Among the serotonin receptor family proteins, the $5HT_{1A}$ receptor ($5HT_{1A}R$) is expressed in the cerebral cortex, hippocampus, amygdala, and raphe nucleus, and mediates inhibitory neurotransmission. $5HT_{1A}R$-knockout ($Htr1a^{-/-}$) mice show elevated-anxiety phenotypes in anxiety paradigms such as the open-field and elevated-plus-maze tests (Heisler et al., 1998;

Parks et al., 1998; Ramboz et al., 1998). In addition to neurotransmitter receptors, many molecular mechanisms (e.g., gene expression, translation, and protein phosphorylation) are involved in higher brain functions. Although intracellular transport controls various aspects of neuronal phenomena, the extent to which intracellular transport is involved in the higher brain functions remains largely unknown. Kinesin superfamily proteins (KIFs) are ATP- and microtubule-dependent molecular motor proteins that control intracellular transport (Hirokawa et al., 2010; Vale, 2003; Verhey and Hammond, 2009). Recent studies showed the involvement of KIFs in some higher brain functions (Kondo et al., 2012; Yin et al., 2011). KIF13A was reported to be a motor protein that transports the mannose-6-phosphate receptor in fibroblasts (Nakagawa et al., 2000). KIF13A is also involved in cytokinesis and endosome-to-melanosome transport in melanocytes (Delevoye et al., 2009; Sagona et al., 2010). Although KIF13A was originally identified from the brain complementary DNA (cDNA) library, the role of KIF13A in neuronal cells remains elusive. For this study, we generated KIF13A knockout ($Kif13a^{-/-}$) mice and analyzed the function of KIF13A in vivo. $Kif13a^{-/-}$ mice showed elevated-anxiety phenotypes in behavioral analyses. We present biochemical and cell biological evidence that KIF13A transports the $5HT_{1A}R$ in neurons. This report suggests the importance of a molecular motor in mood control.

RESULTS

Generation of $Kif13a^{-/-}$ Mice

We performed homologous recombination in embryonic stem cells using a targeting vector (Figure S1A), and used the targeted embryonic stem cells to generate $Kif13a^{-/-}$ mice. We confirmed correct gene targeting by southern blotting (Figure S1B), genomic PCR (Figure S1C), and western blotting with an anti-KIF13A antibody (Figure 1A). The KIF13A band was diminished in $Kif13a^{-/-}$ brain lysate (Figure 1A). KIF13A was originally identified from a brain cDNA library and abundantly expressed in the brain (Nakagawa et al., 1997). To test whether KIF13A is expressed in neurons, we fixed cultured hippocampal neurons and stained them with an anti-KIF13A antibody. To exclude nonspecific signal, the antibody was preabsorbed by acetone powder made from $Kif13a^{-/-}$ tissues. We observed positive fluorescent signal in the cytoplasm of hippocampal neurons (Figures 1B and 1C). No signal was detected in $Kif13a^{-/-}$ neurons
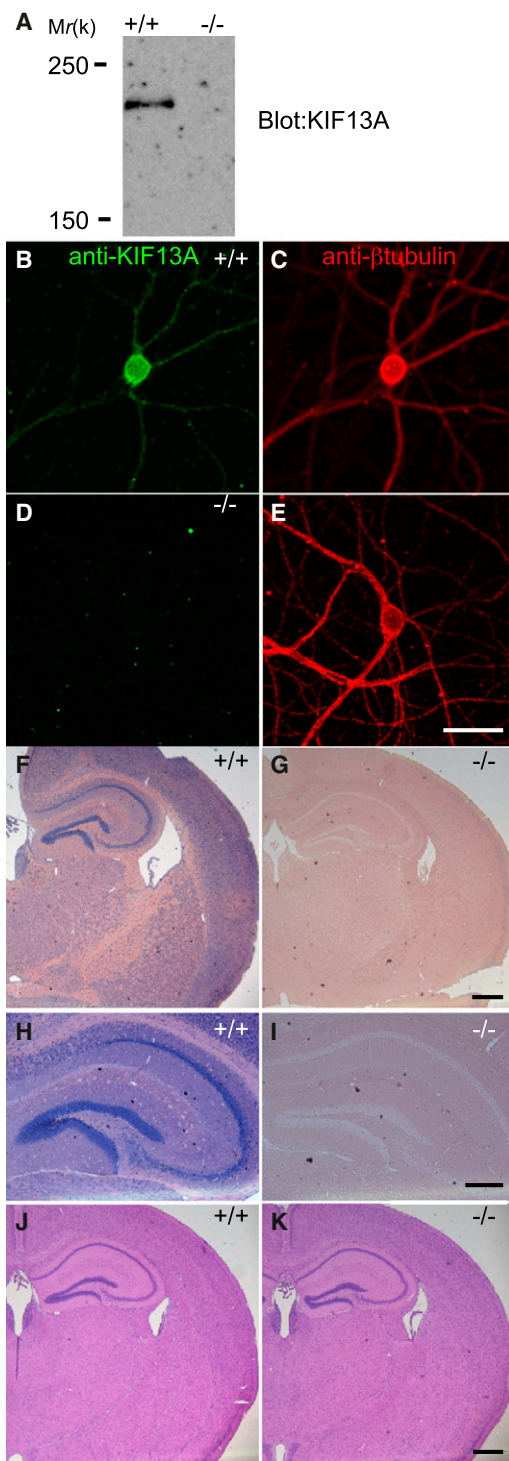
Figure 1. Expression of KIF13A in the Mouse Brain

(A) KIF13A expression was analyzed by western blotting using brain extract from *Kif13a^{+/+}* (+/+) and *Kif13a^{−/−}* (−/−) mice. An anti-KIF13A antibody was used.

(B–E) Hippocampal neurons from *Kif13a^{+/+}* (B and C) and *Kif13a^{−/−}* (D and E) mice, cultured for 12 days, were fixed and stained with an anti-KIF13A antibody that was preabsorbed with acetone powder made from *Kif13a^{−/−}* tissues (B and D). The neuronal cytoplasm was stained. Neurons were

(Figures 1D and 1E). The *Kif13a^{−/−}* mice developed and grew normally (Figure S1D). Nuclear staining revealed that the number of multinucleated cells was not increased (Figures S1F–S1K), which is not consistent with previous results from KIF13A-knockdown experiments (Sagona et al., 2010). The localization of β-adaptin and the mannose-6-phosphate receptor was unaltered in *Kif13a^{−/−}* fibroblasts (Figures S1L–S1O). Furthermore, the coat color, which is a good marker of melanocyte function, was unaffected (Figure S1D). Because the expression of KIF13A was detected in cultured hippocampal neurons, we performed in situ hybridization to reveal the distribution of KIF13A in the brain. We observed that KIF13A was broadly expressed in the hippocampus, thalamus, and cortex (Figure 1F). *Kif13a^{−/−}* brain tissue served as a negative control (Figure 1G). We observed strong expression of KIF13A in the hippocampus (Figures 1H and 1I); however, the brain morphology in KIF13A-knockout mice was unaffected (Figures 1J, 1K, and S1P–S1W).

Kif13a^{−/−} Mice Show Abnormal Responses in Anxiety Paradigms

Although KIF13A is broadly expressed in neurons, the *Kif13a^{−/−}* mice grew normally without any gross anatomical defects of the brain (Figure 1). Thus, we conducted a series of behavioral analyses. In these tests, we detected significant differences between *Kif13a^{−/−}* and wild-type (WT) mice in open-field and elevated-plus-maze tests (Figure 2). In the open-field test, mice were placed in an open field and their behavior was observed. *Kif13a^{−/−}* mice were less active than WT mice in terms of the total distance traveled (40.12 ± 3.74 m and 28.03 ± 2.26 m, respectively; mean $\pm$ SEM, $p < 0.05$, t test; Figure 2A). The *Kif13a^{−/−}* mice entered into the central region less often than the WT mice ($10.12\% \pm 0.64\%$ and $6.42\% \pm 0.33\%$, respectively; mean $\pm$ SEM, $p < 0.05$, t test; Figure 2B). The *Kif13a^{−/−}* mice spent less time in the center of the open field compared with the WT mice ($7.01\% \pm 0.89\%$ and $2.98\% \pm 0.23\%$, respectively; mean $\pm$ SEM, $p < 0.05$, t test; Figure 2C). The *Kif13a^{−/−}* mice also spent less time crossing the center than the WT mice (1.90 ± 0.17 s and 1.41 ± 0.14 s, respectively; mean $\pm$ SEM, $p < 0.05$, t test; Figure 2D). These data indicate that *Kif13a^{−/−}* mice demonstrate higher anxiety than WT mice. In the elevated-plus-maze test, *Kif13a^{−/−}* mice spent significantly less time in the open arms than the WT mice (26.96 ± 1.97 s and 16.83 ± 3.00 s, respectively; mean $\pm$ SEM, $p < 0.05$, t test; Figure 2E). In addition, *Kif13a^{−/−}* mice entered the open arms less frequently than the WT mice (5.42 ± 0.71 times and 3.42 ± 0.42 times, respectively; mean $\pm$ SEM, $p < 0.05$, t test; Figure 2F). One possible explanation for these results is that motor and spatial coordination is affected by the loss of KIF13A. We used

counterstained with the neuronal marker β3-tubulin (C and E). The scale bar indicates 50 μm.

(F–I) In situ hybridization was performed using *Kif13a*-antisense riboprobes on *Kif13a^{+/+}* (+/+) (F and H) and *Kif13a^{−/−}* (−/−) mouse brains (G and I). Scale bars indicate 500 μm and 160 μm, respectively.

(J and K) Brains dissociated from 8-week-old mice were fixed, sectioned, and stained with H&E. Representative images of sections from *Kif13a^{+/+}* (J) and *Kif13a^{−/−}* (K) mice are shown. Scale bars indicate 500 μm.
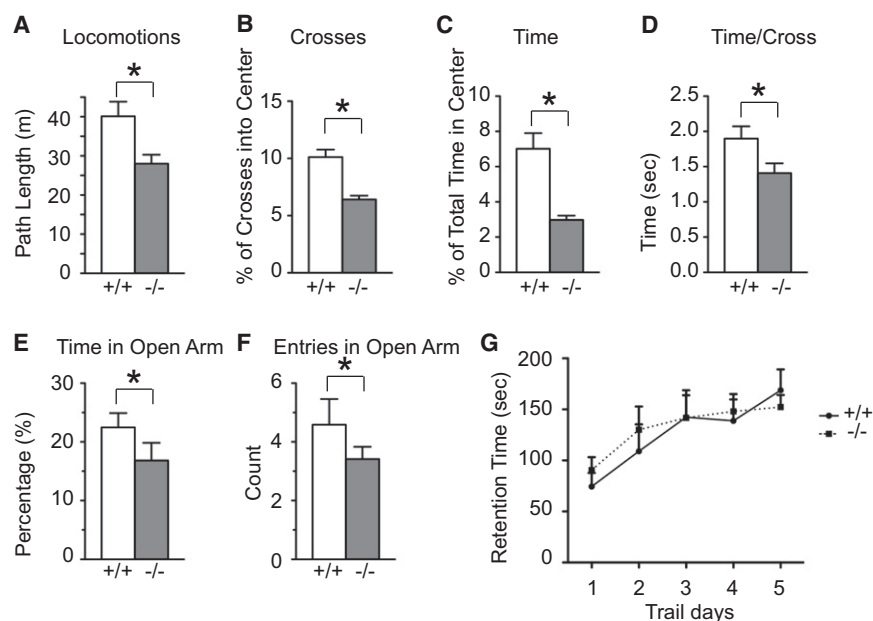
See also Figure S1.

Figure 2. Kif13a^{−/−} Mice Show Elevated-Anxiety Phenotypes

(A–D) Open-field test. (A) The total distance traveled in 10 min was normalized to locomotor activity; $Kif13a^{-/-}$ mice were less active than $Kif13a^{+/+}$ mice. (B) The number of center crosses was normalized to locomotor activity and expressed as the percentage of total crosses; $Kif13a^{-/-}$ mice entered the center less frequently than $Kif13a^{+/+}$ mice. (C) Time spent in the center of the test apparatus is expressed as the percentage of total time (10 min); $Kif13a^{-/-}$ mice spent significantly less time in the center than $Kif13a^{+/+}$ mice. (D) Time per cross indicates the average time spent in the center of the open field for each entry; time spent in the center (time per cross) was lower in $Kif13a^{-/-}$ mice than in $Kif13a^{+/+}$ mice. Data were collected from 12 $Kif13a^{+/+}$ and 10 $Kif13a^{-/-}$ male mice. *$p < 0.05$, mean ± SEM, t test.

(E and F) Elevated-plus-maze test. A significant effect of genotype was found for the time spent in the open arms (E) and the number of entries into the open arms (F). *$p < 0.05$, mean ± SEM, t test for 12 $Kif13a^{+/+}$ and 12 $Kif13a^{-/-}$ male mice.

(G) Rotarod test. Retention time on the rotarod of 6-month-old mice in five successive trials. There was no difference in retention time between WT and $Kif13a^{-/-}$ mice (n = 12, mean ± SEM, one-way ANOVA).

performance on a rotarod test to assess this possibility (Hamm et al., 1994). The rotarod test showed no difference between $Kif13a^{-/-}$ and WT mice over five consecutive days of training (Figure 2G), suggesting that there was no muscle weakness or lack of motor coordination in $Kif13a^{-/-}$ mice. These behavioral tests showed that a deficiency of KIF13A leads to an elevated-anxiety phenotype without affecting motor coordination.

Distribution of 5HT_{1A}Rs in Kif13a^{−/−} Neurons

The results described above suggest that $Kif13a^{-/-}$ mice have an elevated-anxiety phenotype. Many studies have shown that defects in the 5-HT pathway lead to such phenotypes. We postulated that 5-HT synthesis and/or release were reduced in the $Kif13a^{-/-}$ brain. To test this, we used ELISAs to compare the amount of 5-HT in WT and $Kif13a^{-/-}$ brain lysates, and in medium conditioned by WT or $Kif13a^{-/-}$ neurons. No significant differences were detected (Figure 3A). Previous studies showed that $Htr1a^{-/-}$ mice also demonstrate high-anxiety phenotypes (Heisler et al., 1998; Parks et al., 1998; Ramboz et al., 1998) that are similar to those observed in $Kif13a^{-/-}$ mice. Hence, we compared the amount of 5HT$_{1A}$R protein localized on plasma membranes of WT and $Kif13a^{-/-}$ neurons using an antibody that recognizes an extracellular domain of the 5HT$_{1A}$R (Azmitia et al., 1992; Figure 3B). The antibody was prepared as described previously, and recognized a 65-kDa protein by western blotting (Figure S2A), consistent with previous studies (Raymond et al., 1993a; Zhou et al., 1999). Because 5HT$_{1A}$R is glycosylated in cells, the molecular weight is higher than the predicted size. We studied the 5HT$_{1A}$R in cultured hippocampal neurons because its expression in the forebrain, mainly in hippocampal neurons, can rescue $Htr1a^{-/-}$ phenotypes (Gross et al., 2002). Compared with WT neurons, the labeling intensity was signifi-

cantly decreased in $Kif13a^{-/-}$ neurons (Figures 3C–3E). When we compared the total expression levels of the 5HT$_{1A}$R by western blotting, we found no significant difference (Figures 3F, S2A, and S2B). We then compared the cell-surface expression of 5HT$_{1A}$Rs in primary hippocampal neurons derived from WT and $Kif13a^{-/-}$ embryos. The cell-surface expression of 5HT$_{1A}$Rs was significantly reduced in $Kif13a^{-/-}$ neurons, whereas that of GluR3 was not changed (Figures 3F and 3G). Another anti-5HT$_{1A}$R antibody, which recognizes a different antigen in the 5HT$_{1A}$R, was used in a cell-surface assay and confirmed that the cell-surface expression of 5HT$_{1A}$Rs was reduced in $Kif13a^{-/-}$ neurons (Figure S2C). These data suggest that the surface expression of the 5HT$_{1A}$R, but not the total expression level, is changed in $Kif13a^{-/-}$ neurons.

Effects of 5-HT Receptor Agonists and Antagonists on Kif13a^{−/−} Neurons

Serotonin receptors are seven-transmembrane domain receptors. These 5-HT receptors, with the exception of the 5-HT$_3$ receptor, are G protein coupled. 5-HT receptors stimulate or inhibit the production of cyclic AMP (cAMP). Previous studies showed that the 5HT$_{1A}$R agonist 8-Hydroxy-2-(di-n-propyla-mino)tetralin hydrobromide (8-OH-DPAT) stimulates the production of cAMP in hippocampal neurons, although the 5HT$_{1A}$R is associated with the Gi alpha subunit (Cadogan et al., 1994; Raymond et al., 1993b). This is caused by the specific cellular environment of hippocampal neurons (Roth, 2006). Thus, the cell-surface level of 5HT$_{1A}$R can be monitored by comparing the intracellular levels of cAMP in the presence or absence of 5-HT$_{1A}$R agonists and antagonists in cultured hippocampal neurons. Basal cAMP accumulation in primary hippocampal neurons amounted to 18.79 ± 0.72 pmol/ml and
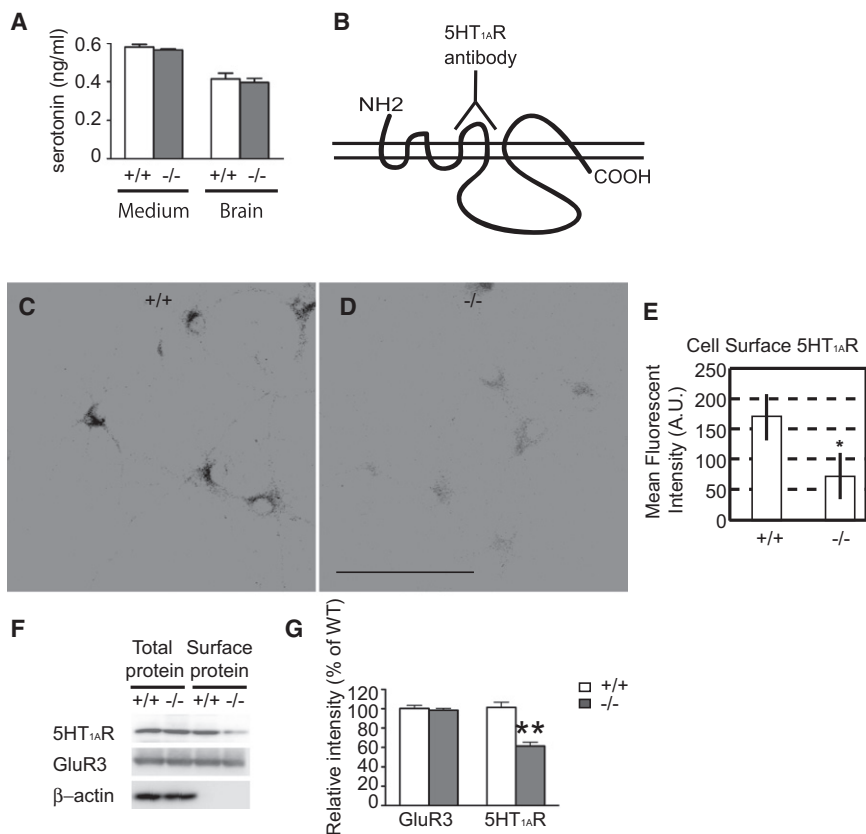
Figure 3. Expression of the 5HT$_{1A}$R Is Reduced at the Plasma Membrane

(A) ELISAs were performed to compare the amount of 5-HT in brain lysate and medium conditioned with cultured neurons. There were no differences in the total amount in the brain or in secreted 5-HT levels in cultured neurons between WT and *Kif13a*$^{-/-}$ mice (n = 5, t test, mean ± SEM). Left: Secreted 5-HT from the medium of primary-cultured hippocampal cells. Right: Secreted 5-HT from brain homogenates.

(B) A schematic showing the structure of the 5HT$_{1A}$R and the antigen. The antibody is able to recognize the cell-surface 5HT$_{1A}$R.

(C and D) Cultured hippocampal neurons dissociated from a *Kif13a*$^{+/+}$ brain (C) and a *Kif13a*$^{-/-}$ brain (D) were fixed and stained with the anti-5HT$_{1A}$R antibody without detergent extraction. The scale bar indicates 100 μm.

(E) Quantification of mean fluorescent density. The data are shown as mean ± SD, *p < 0.01, mean ± SEM, t test, n = 30.

(F) Cell-surface expression of proteins in *Kif13a*$^{+/+}$ and *Kif13a*$^{-/-}$ hippocampal neurons. Proteins that were exposed on the plasma membrane of cultured hippocampal neurons were biotinylated and purified. Proteins were analyzed by western blotting. The amount of cell-surface 5HT$_{1A}$R was significantly reduced in *Kif13a*$^{-/-}$ hippocampal neurons, whereas that of GluR3 was unchanged. Beta-actin, which is not exposed on the cell surface, was used as a purification marker.

(G) Statistical analysis of the cell surface expression in (F). The absence of intracellular protein (actin) signals verifies the purity of the cell-surface protein fraction. *p < 0.05, mean ± SEM, t test, n = 5.

See also Figure S2.

20.03 ± 1.97 pmol/ml (mean ± SEM, n = 6), respectively, in WT and *Kif13a*$^{-/-}$ neurons; there was no significant difference between them. Application of 8-OH-DPAT increased cAMP formation in WT neurons by ∼15% (1 μM), 19.8% (10 μM), and 25.6% (100 μM) in a dose-dependent manner, but it did not significantly increase cAMP formation in *Kif13a*$^{-/-}$ neurons (Figure 4A). The 5HT$_{1A}$R antagonist WAY-100635 had no significant effect on cAMP levels in either WT or *Kif13a*$^{-/-}$ neurons even at high concentration (100 μM; Figure 4B). This is probably because cultured neurons are not stimulated by endogenous serotonin (Ramboz et al., 1998). We also tested other serotonin receptor agonists and antagonists. There was no difference between WT and *Kif13a*$^{-/-}$ neurons when we stimulated primary hippocampal cultures with the 5HT$_{1B}$ agonist CP-93129 (Figure S3A), the 5HT$_{1B}$ antagonist GR-55562 (Figure S3B), or the 5HT$_{2A/2C}$ agonist ketanserin (Figure S3C). To assess whether the elevated-anxiety phenotype of *Kif13a*$^{-/-}$ mice results from the 5HT$_{1A}$R pathway, we compared the effects of 8-OH-DPAT and WAY-100635 in the open-field test. We found no significant effects of 8-OH-DPAT (at 0.1 mg/kg and 1.0 mg/kg) on either WT or *Kif13a*$^{-/-}$ mice (Figure 4C). It has been shown that 8-OH-DPAT has no effect even on WT behavior in this test because the serotonin receptors are saturated by endogenous serotonin in this condition (Ramboz et al., 1998). In contrast, both doses of WAY-100635 (0.03 mg/kg and 0.3 mg/kg) resulted

in a significant decrease in time spent in the center of the open field by WT mice. However, WAY-100635 caused no significant effect in *Kif13a*$^{-/-}$ mice (Figure 4D). These results are similar to those observed in *Htr1a*$^{-/-}$ mice, suggesting that the function of 5HT$_{1A}$R is affected in *Kif13a*$^{-/-}$ hippocampal cells and the behavioral abnormality in the open-field test is caused by the defect of the 5HT$_{1A}$R.

The Forkhead-Associated Domain of KIF13A Binds to an Intracellular Loop of the 5HT$_{1A}$R

Behavioral phenotypes, pharmacological assays, and surface labeling assays all suggested that the 5HT$_{1A}$R was altered in *Kif13a*$^{-/-}$ neurons. Because KIF13A is a molecular motor, we tested the hypothesis that the 5HT$_{1A}$R is a cargo of KIF13A in neurons. First, we performed immunoprecipitation in the presence of the detergent 3-[(3-cholamidopropyl)dimethylammonio]-1-propanesulfonate (CHAPS). The 5HT$_{1A}$R could be copurified with KIF13A in the presence of 0.3% CHAPS (Figure 5A), suggesting an association between the two. To test this, we used yeast two-hybrid assays using an intracellular domain of the 5HT$_{1A}$R and deletion mutants of KIF13A and the 5HT$_{1A}$R cloned into yeast two-hybrid vectors (Figure 5B). The Y2HGold strain of yeast was transformed with these vectors and plated onto selection plates containing 5-bromo-4-chloro-3-indolyl α-D-galactopyranoside (X-α-gal). The results suggested that the intracellular
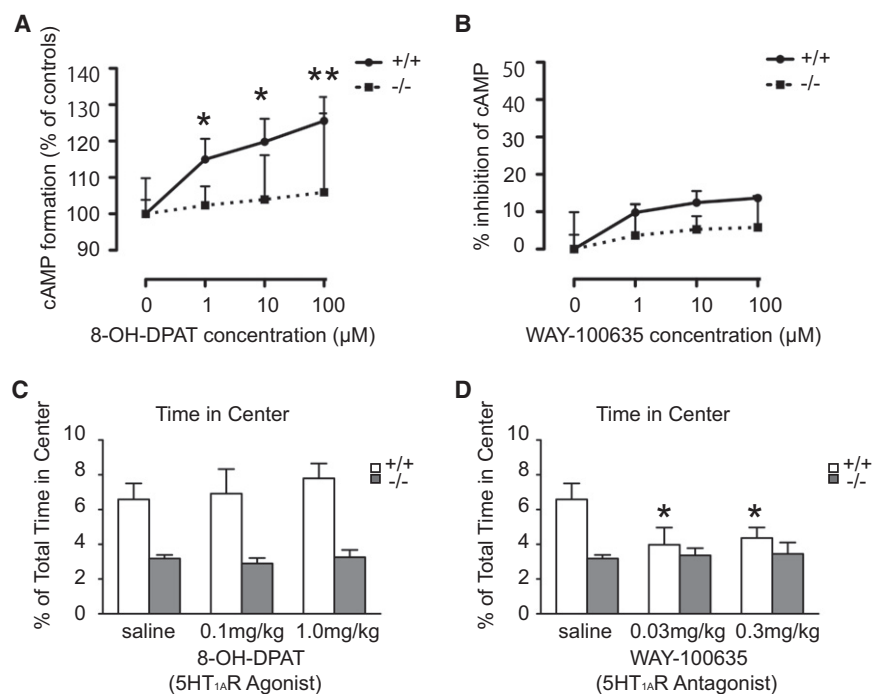
Figure 4. Pharmacological Analysis

(A and B) Effects of 8-OH-DPAT (A) and WAY-100635 (B) on cellular cAMP formation in cultured hippocampal neurons. 8-OH-DPAT stimulated cAMP formation with a dose-response relationship (A). WAY-100635 did not completely inhibit cAMP formation (B). The effects are expressed as the percentage of basal cAMP formation. *$p < 0.05$, mean ± SEM, t test, n = 6.

(C and D) Effect of 8-OH-DPAT (C) and WAY-100635 (D) in the open-field test. There was no significant effect of 8-OH-DPAT on $Kif13a^{+/+}$ or $Kif13a^{-/-}$ mice (C). Although there was a significant effect of WAY-100635 on $Kif13a^{+/+}$ mice in terms of the mean time spent in the center of the open field, this antagonist had no effect on $Kif13a^{-/-}$ mice (D). *$p < 0.05$, mean ± SEM, n = 10, two-way ANOVA.

See also Figure S3.

loop of the 5HT$_{1A}$R interacts directly with the forkhead-associated (FHA) domain of KIF13A (FHA^{KIF13A}; amino acids 420–604 of KIF13A; Figure 5C). To confirm binding via the FHA domain, we conducted glutathione-S-transferase (GST) pull-down assays using FHA^{KIF13A} as bait. The FHA domain of KIF1B (FHA^{KIF1B}; amino acids 455–629 of KIF1B) was used as a negative control. GST-FHA^{KIF13A} and GST-FHA^{KIF1B} were expressed in *Escherichia coli* and bound to glutathione-sepharose beads. The beads were incubated with brain lysate, washed, and then analyzed by SDS-PAGE and western blotting using an anti-5HT$_{1A}$R antibody. The GST-FHA^{KIF13A} beads could precipitate the 5HT$_{1A}$R, but the GST-FHA^{KIF1B} beads could not (Figure 5D). Other 5-HT receptors could not be purified by GST-FHA^{KIF13A}-conjugated beads. We confirmed the binding of the KIF13A full-length fragment and FHA domain with the 5HT$_{1A}$R by Flag-tag immunoprecipitation (Figure 5E). These results suggest that the 5HT$_{1A}$R is transported by KIF13A probably by direct binding. To confirm that FHA^{KIF13A} is involved in the transport of 5HT$_{1A}$Rs, we performed knockdown and rescue experiments in SK-N-SH human neuroblastoma cells. SK-N-SH cells were chosen because they endogenously express the 5HT$_{1A}$R (Fricker et al., 2005); also, the cells are flat, which makes it easy to visualize the plasma membrane localization of the 5HT$_{1A}$R. Using microRNA (miRNA) vectors against human KIF13A, we knocked down endogenous KIF13A expression in SK-N-SH neuroblastoma cells. By western blotting, its expression was reduced to ~40% of WT levels (Figure 5F). Because the transfection efficiency was ~70%, we thought that the knockdown was sufficient. Then, we used a vector encoding a green fluorescent protein (GFP)-5HT$_{1A}$R fusion protein to monitor the localization of the 5HT$_{1A}$R. Previous studies have shown that the GFP-fused 5HT$_{1A}$R is fully functional and mimics the localization of the

endogenous 5HT$_{1A}$R (Renner et al., 2007; Carrel et al., 2008; Ghavami et al., 1999). We cotransfected the GFP-5HT$_{1A}$R vector with the miRNA vectors and incubated them for 3 days. The cells were then fixed and observed. The GFP-5HT$_{1A}$R was localized to the plasma membrane in control cells; however, this receptor accumulated on vesicular structures around the nucleus in KIF13A-knockdown cells (Figures 5G–5I). Two independent and different knockdown vectors were able to induce this effect reproducibly. To show the importance of the association between the 5HT$_{1A}$R and FHA^{KIF13A} by a cell biological method, we cotransfected Flag-tagged full-length mouse KIF13A (KIF13Afull), the motor domain of KIF13A (KIF13A420; amino acids 1–420 of KIF13A), and a minimotor consisting of the motor domain and FHA^{KIF13A} (KIF13A604; amino acids 1–604 of KIF13A) into KIF13A-knockdown cells. Because these constructs were made from mouse source material, they were nonreactive to human miRNA vectors and were expressed normally (Figure 5J). When Flag-KIF13Afull and Flag-KIF13A604 were expressed, the GFP-5HT$_{1A}$R was localized on the plasma membrane (Figures 5K and 5M). In contrast, when Flag-KIF13A420 was expressed, the GFP-5HT$_{1A}$R accumulated on vesicles around the nucleus (Figure 5L). Collectively, these data suggest that the FHA domain of KIF13A associates with the 5HT$_{1A}$R, and that the interaction is essential for the transport of this receptor.

Intracellular Transport of the 5HT$_{1A}$R in $Kif13a^{-/-}$ Neurons

We observed the intracellular transport of the 5HT$_{1A}$R by expressing the GFP-5HT$_{1A}$R fusion protein in hippocampal neurons. Forty-eight hours after transfection, whereas the GFP-5HT$_{1A}$R in WT neurons was localized mainly to the plasma membrane, the GFP-5HT$_{1A}$R in $Kif13a^{-/-}$ neurons was concentrated in a perinuclear structure (Figures 6A–6H). This structure partially colocalized with the Golgi marker GM130 (Figures 6E–6H). The accumulation was not observed in WT neurons.
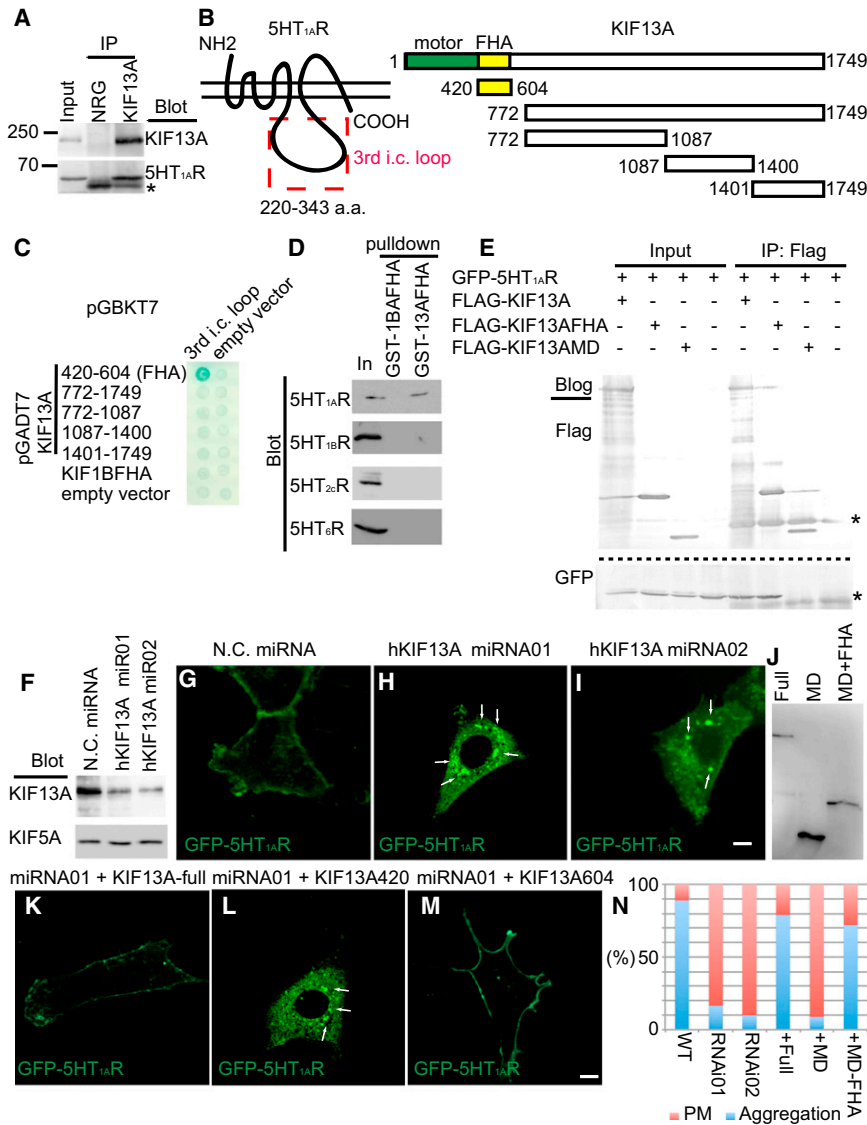
Figure 5. The FHA Domain of KIF13A Binds to the Intracellular Loop of the 5HT₁ₐR

(A) Immunoprecipitation was performed using normal anti-rabbit IgG (NRG) and the anti-KIF13A antibody (KIF13A). Input and immunoprecipitated fractions (IP) were separated by SDS-PAGE, transferred to a membrane, and blotted with the anti-KIF13A and anti-5HT₁ₐR antibodies. The asterisk indicates the IgG bands.

(B) Schematic showing the structure of the 5HT₁ₐR and KIF13A.

(C) Yeast two-hybrid assays. A positive signal (blue) was obtained between the FHA domain of KIF13A and the intracellular domain of the 5HT₁ₐR.

(D) GST pull-down assay. GST-FHA^KIF1B and GST-FHA^KIF13A were expressed in *E. coli* and adsorbed to glutathione beads. The beads were incubated with brain lysate, washed, and analyzed by western blotting using the anti-5HT₁ₐR antibody.

(E) Neuro2A cells were transfected with the indicated constructs and immunoprecipitated with anti-Flag antibody. Beads were subjected to western blot analysis with anti-Flag and anti-GFP antibodies. Left panel: KIF13A constructs used in this study. Right panel: A representative result of three independent western blot experiments. * IgG band.

(F–I) A vector encoding the GFP-5HT₁ₐR was cotransfected into SK-N-SH human neuroblastoma cells with a negative control vector (N.C.) or two human KIF13A-miRNA vectors (hKIF13A miRNA01 and hKIF13A miRNA02), cultured for 3 days, and fixed. The scale bar indicates 100 μm.

(J–M) SK-N-SH cells were transfected with the GFP-5HT₁ₐR, hKIF13A-miRNA01, and Flag-tagged mouse KIF13A mutants, cultured for 3 days, and then fixed. Blotting shows the expression of full-length KIF13A, KIF13A420, and KIF13A604. The scale bar indicates 100 μm.

(N) The number of cells with plasma membrane localization of the 5HT₁ₐR or cells with perinuclear aggregation of 5HT₁ₐR was counted and is shown graphically. n = 30 cells from three independent transfections.

Moreover, it could be rescued by overexpression of the KIF13A-full fragment and KIF13A604, but not by KIF13A420 (Figure S4). Next, we performed live-cell imaging of 5HT₁ₐR transport in neurons. To observe transported vesicles, we observed neurons 8–12 hr after transfection. It was previously shown that the 5HT₁ₐR is exclusively localized to dendrites in hippocampal neurons (Ghavami et al., 1999). Thus, we anticipated that the 5HT₁ₐR was transported from the cell body to dendrites by vesicular carriers, as is the case for other neuronal receptors (Guillaud et al., 2003). However, we observed no anterograde vesicular movement in dendrites, even in WT neurons (Movie S1; n = 60 immature and 60 mature neurons; total observation time was ~20 hr). To reduce the background and improve the observation, we performed fluorescence recovery after photobleaching (FRAP; Nakata et al., 1998). Although anterograde vesicular transport was not observed, we did observe the GFP-5HT₁ₐR moving by diffusion onto the dendritic plasma membrane (Movie S2). Next, we tried to observe the motility of the GFP-5HT₁ₐR-positive organelles in the cell body. Tubular structures moving to the plasma membrane were seen in 5-day-old WT neurons, 12 hr after transfection (Movie S3). The speed of these organelles was 0.5 ± 0.2 μm/s (n = 25). These organelles sometimes collided with the plasma membrane, diminished rapidly, and caused the plasma membrane to expand (Movie S4; Figure 6I). We believe that transported organelles fuse with the plasma membrane, and that the GFP-5HT₁ₐR diffuses rapidly on the plasma membrane. In contrast, in *Kif13a^−/−* cells, GFP-5HT₁ₐR-containing vesicles tended to accumulate around the cell body. The motility of the GFP-5HT₁ₐR was significantly reduced, and the number of 5HT₁ₐR-carrying organelles that collided with the plasma membrane was significantly reduced compared with that in WT cells (Movie S3; Figures 6J and 6K). These data suggest that the 5HT₁ₐR is transported to the plasma membrane in the cell body, and that the molecular motor is
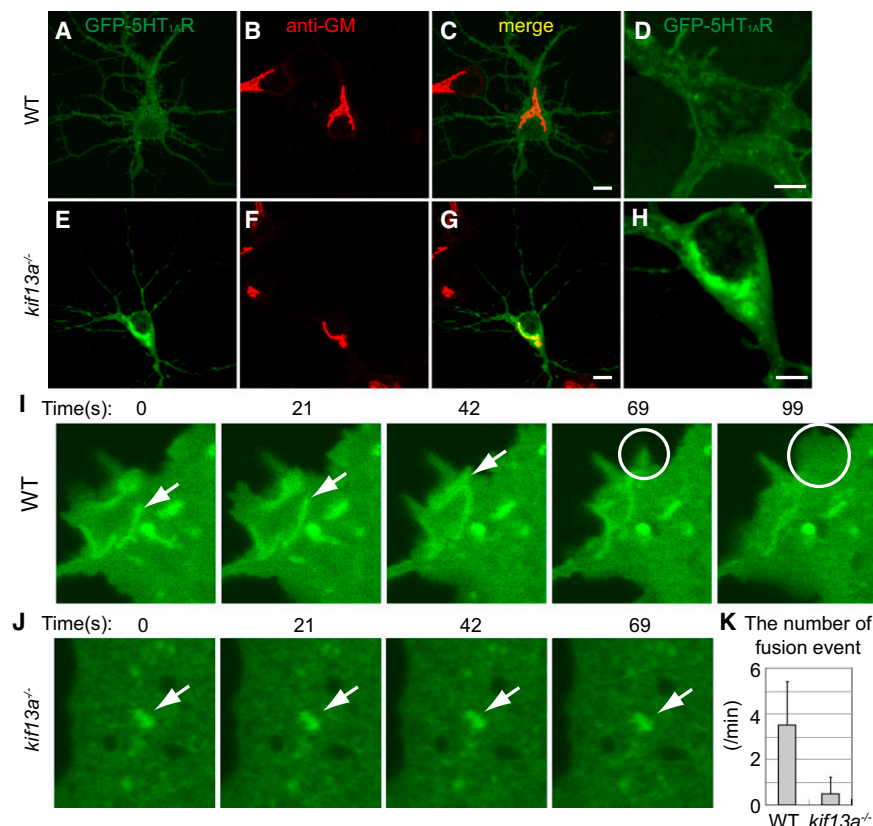
Figure 6. Intracellular Transport of the 5HT$_{1A}$R

(A–H) The GFP-5HT$_{1A}$R (green) was expressed in Kif13a$^{+/+}$ (A–D) and Kif13a$^{-/-}$ (E–H) neurons. The neurons were fixed and then stained with a marker for the Golgi apparatus (GM130, red).

(I and J) Live-cell imaging of the GFP-5HT$_{1A}$R (green) in Kif13a$^{+/+}$ (I) and Kif13a$^{-/-}$ (J) neurons. Representative still images are shown in (I) and (J).

(K) Number of GFP-5HT$_{1A}$R-positive organelles that fused with the plasma membrane. The data are shown as mean ± SD, n = 11 Kif13a$^{+/+}$ and Kif13a$^{-/-}$ cells from three independent cultures. See also Figure S4, and Movies S1, S2, S3, S4, S6, and S7.

KIF13A. To test whether other vesicular markers were affected in Kif13a$^{-/-}$ neurons, we overexpressed GFP-fused glutamate-binding N-methyl-D-aspartate receptor subunit type 2B (GFP-NR2B) in primary cultured hippocampal neurons. Time-lapse recordings revealed that most GFP-NR2B clusters were moving along dendrites in WT and Kif13a$^{-/-}$ neurons. There was no significant difference in the classification of motility (nonmobile, vibrating, anterograde, and retrograde) between WT and Kif13a$^{-/-}$ neurons (Figure S4J; Movies S6 and S7). Furthermore, there was no significant difference in the velocity of anterogradely or retrogradely transported GFP-NR2B clusters between WT and Kif13a$^{-/-}$ neurons (Figure S4K; Movies S6 and S7).

In Vitro Reconstitution of 5HT$_{1A}$R Transport

Finally, to confirm that the 5HT$_{1A}$R is transported by KIF13A through the FHA domain, we performed in vitro reconstitution experiments (Nangaku et al., 1994). KIF13A420 and KIF13A604 were cloned into the pET28a vector, expressed in E. coli, and purified (Figure 7A). Vesicular fractions containing GFP-5HT$_{1A}$R were purified using density gradients. To exclude the possibility that endogenous KIF13A would affect the results, GFP-5HT$_{1A}$R vesicles were prepared from Kif13a$^{-/-}$ fibroblasts. Both KIF13A420 and KIF13A604 could translocate microtubules in the microtubule-gliding assay, as described previously (Nakagawa et al., 2000). The gliding speed of both KIF13A420 and KIF13A604 was 0.8 ± 0.2 μm/s (mean ± SD) in >30 microtubules, suggesting that these recombinant proteins have motor activity. We investigated whether these minimotors can transport GFP-

5HT$_{1A}$R vesicles onto microtubules in vitro. Taxol-stabilized microtubules labeled with biotin and tetramethylrhodamine were fixed onto avidin-coated coverslips, and motility buffer containing GFP-5HT$_{1A}$R vesicles, purified motors, and nucleotides were added to the chamber (Figure S5). KIF13A604 could translocate GFP-5HT$_{1A}$R vesicles (Movie S5; Figures 7B and 7C). The speed of vesicle movement was 0.7 ± 0.3 μm/s (mean ± SD, n = 50 tubules and vesicles), which is consistent with the results from the microtubule gliding assay. We also observed the movement of both vesicular and tubular organelles in vitro (Figure 7B). When KIF13A420 was coincubated with vesicles, no vesicular movement was observed. These in vitro assay data support our findings that KIF13A transports 5HT$_{1A}$R-carrying vesicles in neurons, and the FHA domain is the cargo-binding domain.

DISCUSSION

Anxiety Control by a Molecular Motor

Because anxiety is a complex higher brain function and is clinically important, its molecular mechanisms have been studied intensively. Previous studies have demonstrated the roles of neurotransmitters, receptors, and downstream signaling in anxiety control (Chen et al., 2001; Hendricks et al., 2003; Park et al., 2005; Parks et al., 1998; Ramboz et al., 1998). Little attention has been given to the role of molecular motors and intracellular transport in this process, although recent studies have revealed that molecular motors regulate higher brain functions such as learning and memory through intracellular transport (Kondo et al., 2012; Yin et al., 2011). On the basis of the work presented here, we suggest that the molecular motor KIF13A is fundamental to anxiety control. Kif13a$^{-/-}$ mice showed elevated-anxiety phenotypes in the open-field and elevated-plus-maze tests. Considering that KIF13A has been shown to be involved in AP-1-dependent mannose-6-phosphate receptor transport (Nakagawa et al., 2000), cytokinesis (Sagona et al., 2010), and endosome-to-melanosome transport
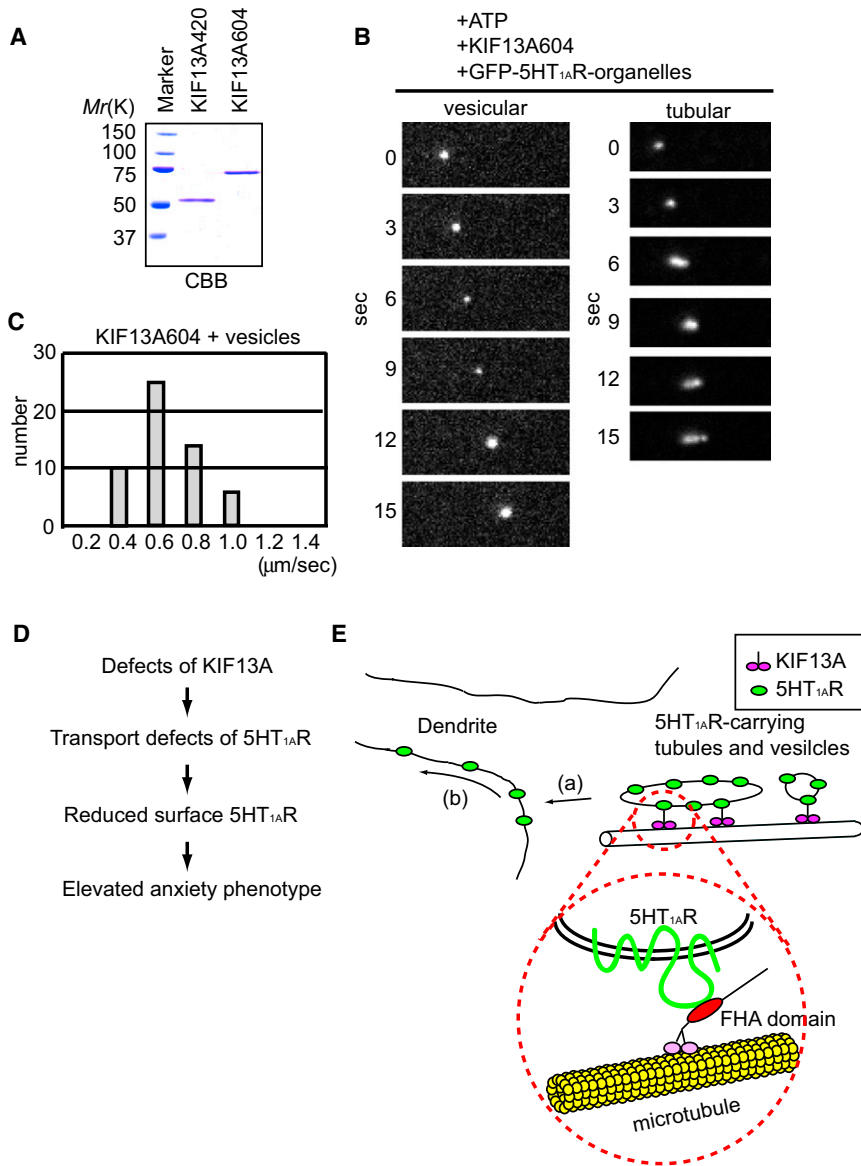
A

Mr(K) Marker KIF13A420 KIF13A604

150
100
75
50
37

CBB

B

+ATP
+KIF13A604
+GFP-5HT$_{1A}$R-organelles

vesicular   tubular

sec 0, 3, 6, 9, 12, 15   sec 0, 3, 6, 9, 12, 15

C

KIF13A604 + vesicles

number
30
20
10
0
0.2 0.4 0.6 0.8 1.0 1.2 1.4
(μm/sec)

D

Defects of KIF13A
↓
Transport defects of 5HT$_{1A}$R
↓
Reduced surface 5HT$_{1A}$R
↓
Elevated anxiety phenotype

E

KIF13A
5HT$_{1A}$R

Dendrite

5HT$_{1A}$R-carrying
tubules and vesilces

(a)
(b)

5HT$_{1A}$R

FHA domain

microtubule

Figure 7. In Vitro Reconstitution Experiments

(A–C) Recombinant motors and GFP-5HT$_{1A}$R organelles were purified from *E. coli* and *Kif13a$^{-/-}$* fibroblasts, respectively. Tetramethylrhodamine- and biotin-labeled microtubules were fixed on avidin-coated glass coverslips. Purified motors, vesicles, and nucleotides were mixed and dispensed onto the coverslips. Time-lapse observation was performed using TIRF.

(A) Gel image showing the purification of recombinant motors.

(B) Still images showing the motility of the GFP-5HT$_{1A}$R-carrying organelles in vitro.

(C) Speed of the GFP-5HT$_{1A}$R-carrying organelles. The motility was observed only when KIF13A604 was mixed with 5 mM ATP. The data are shown as mean ± SD, n = 27.

(D) Model for elevated anxiety in *Kif13a$^{-/-}$* mice.

(E) Model for intracellular transport of the 5HT$_{1A}$R in hippocampal neurons. (a) 5HT$_{1A}$R-carrying organelles are transported by KIF13A from the Golgi apparatus to the plasma membrane in the cell body. (b) The 5HT$_{1A}$R diffuses into the dendritic plasma membrane.

See also Figure S5 and Movie S5.

(Delevoye et al., 2009), it was possible that an absence of, or defects in, these processes might cause the elevated anxiety. However, we could not detect differences in these phenomena in *Kif13a$^{-/-}$* mice, probably owing to functional compensation by other motors (e.g., KIF5, which also binds to and transports the AP-1 complex; Schmidt et al., 2009). Many studies have shown that a single motor transports several cargos, and vise versa (Hirokawa et al., 2010; Vale, 2003; Verhey and Hammond, 2009). Here, we demonstrate that the 5HT$_{1A}$R is a cargo of KIF13A. The amount of cell-surface 5HT$_{1A}$ was significantly reduced in *Kif13a$^{-/-}$* neurons, although the total expression level of the 5HT$_{1A}$R and the amount of 5-HT in the brain were not significantly altered. Full-length KIF13A was not required for transport of the 5HT$_{1A}$R. The FHA domain of KIF13A directly associated with the intracellular domain of the 5HT$_{1A}$R in yeast two-hybrid assays. In an in vitro reconstitution assay, we showed that

5HT$_{1A}$R-carrying organelles were translocated by a recombinant minimotor consisting of the motor and FHA domains. The minimotor could rescue mislocalization of the 5HT$_{1A}$R in KIF13A-knockdown cells. This finding is not surprising, because other studies have shown that the full-length KIF is not always required for intracellular transport (Glater et al., 2006; Horiguchi et al., 2006; Kanai et al., 2004). The stalk domain may be involved in the regulation of transport (Verhey and Hammond, 2009). In live-cell imaging experiments, the motility of 5HT$_{1A}$R-carrying organelles was changed in *Kif13a$^{-/-}$* neurons. The 5HT$_{1A}$R was concentrated to perinuclear vesicular structures in *Kif13a$^{-/-}$* neurons and KIF13A-knockdown neuroblastoma cells (Figures 5 and S4). Biochemical interactions, reduced motility, and mislocalization in mutant cells are well-established criteria for determining the motor–cargo relationship (Hall and Hedgecock, 1991; Hirokawa et al., 2010; Niwa et al., 2008; Stowers et al., 2002). Thus, we conclude that the 5HT$_{1A}$R is a cargo of the molecular motor KIF13A. Because the 5HT$_{1A}$R is fundamental to anxiety control (Gross et al., 2002; Parks et al., 1998; Ramboz et al., 1998), our findings suggest that a reduced amount of cell-surface 5HT$_{1A}$R, due to defects in its intracellular transport, is a cause of the elevated-anxiety phenotypes in *Kif13a$^{-/-}$* mice (Figure 7D).

Intracellular Transport of the 5HT$_{1A}$R

Because the 5HT$_{1A}$R is an important target in the treatment of mood disorders, the biochemical and pharmacological

properties of the 5HT$_{1A}$R have been studied extensively (Gordon and Hen, 2004). However, it remains largely elusive how the 5HT$_{1A}$R is transported. Expression of the 5HT$_{1A}$R in hippocampal and cortical neurons of $Htr1a^{-/-}$ mice can ameliorate abnormal behavior (Gross et al., 2002), and thus cultured hippocampal neurons should be a good model system in which to address this question (Banker and Goslin, 1991; Dotti and Banker, 1991). Using this system, a previous study showed that the 5HT$_{1A}$R is exclusively transported to dendrites, whereas the 5HT$_{1B}$R is transported to both the axons and dendrites in hippocampal neurons (Roth and Xia, 2004). As a mechanism of dendritic transport, other investigators and we have shown that dendritic receptors, such as NR2A and NR2B, are transported from the cell body to dendrites by vesicular transport using a dendrite-specific motor (Chu et al., 2006; Guillaud et al., 2003; Setou et al., 2000). However, this study suggests that intracellular transport of the 5HT$_{1A}$R differs from that of other receptors. In dendrites, we observed only diffusive motion of the 5HT$_{1A}$R on plasma membranes, not vesicular transport (Movies S1 and S2; total observation time was ~20 hr). This suggests that the 5HT$_{1A}$R moves from the cell body to dendrites by diffusion rather than by vesicular transport. The motility of the 5HT$_{1A}$R-carrying organelles was observed mainly in the cell body, and these organelles probably fuse with the plasma membrane in the cell body. The 5HT$_{1A}$R-carrying organelles are mainly tubules in neurons. Tubular carriers are sometimes reported in other cases, such as TrkA receptors, synaptic vesicle precursors, major histocompatibility class II molecules, and recycling endosomes (Chow et al., 2002; Nakata et al., 1998; Weigert et al., 2004). We found that it was technically difficult to stain the tubular organelles with antibodies, as was previously observed (Nakata et al., 1998). However, because the GFP-5HT$_{1A}$R was transported to the plasma membrane and was functional, we believe that these structures reflect the endogenous transport pathway. The 5HT$_{1A}$R was concentrated to perinuclear vesicular structures in $Kif13a^{-/-}$ neurons and KIF13A-knockdown neuroblastoma cells, suggesting that KIF13A is involved in the transport of the 5HT$_{1A}$R from the Golgi apparatus to the plasma membrane. It has been suggested that the 5HT$_{1A}$R is transported by KIF5B via the YIF1B scaffold protein (Al Awabdh et al., 2012; Carrel et al., 2008). Because the 5HT$_{1A}$R is not completely diminished from the plasma membrane in $Kif13a^{-/-}$ neurons, it is possible that KIF5 partially compensates for the function of KIF13A. It is an open question as to how the 5HT$_{1A}$R diffuses specifically from the cell body into the dendritic plasma membrane of hippocampal neurons. One possibility is that there is a diffusion barrier on the plasma membrane of the axon initial segment (Hedstrom et al., 2008; Kobayashi et al., 1992; Nakada et al., 2003). Further studies will be required to elucidate this process. Another unique characteristic of 5HT$_{1A}$R transport by KIF13A is that KIF13A transports the 5HT$_{1A}$R probably by direct binding. Previous studies have shown that KIFs bind to the membrane proteins in cargos through an adaptor protein complex (Horiguchi et al., 2006; Nakagawa et al., 2000; Setou et al., 2000; Wang and Schwarz, 2009). It has been shown that the FHA domain of KIF13B serves as a cargo-binding domain (Horiguchi et al., 2006). Considering that KIF13A transports the mannose-6-phosphate receptor by

the C-terminal tail domain (Nakagawa et al., 2000), our findings suggest a mechanism for how one motor recognizes several cargos.

In conclusion, we have revealed a role for molecular motors in anxiety. The molecular motor KIF13A could be considered a potential pharmaceutical target for anxiolytic drugs.

EXPERIMENTAL PROCEDURES

Gene Targeting of *Kif13a* and Generation of *Kif13a$^{-/-}$* Fibroblasts

All procedures involving animals were approved by the School of Medicine of the University of Tokyo, and conformed to the relevant regulatory standards. A targeting vector was constructed to disrupt the *Kif13a* gene (Figure S1A). *Kif13a$^{+/-}$* mice were obtained by intercrossing the *Kif13a$^{3lox/+}$* mice with CAG-Cre strain mice (kindly provided by J. Miyazaki; Sakai and Miyazaki, 1997). Genotypes were determined by genomic PCR. Immortalization of fibroblasts was achieved by stable transfection with an expression vector containing SV40 large T antigen.

Behavioral Tests

All researchers who performed animal experiments had the required training, and all experiments were conducted under the University of Tokyo's rules regarding animal experimentation. Adult WT and *Kif13a$^{-/-}$* male mice (3- to 9-month-old littermates, n = 12) were used throughout the behavioral tests. ANOVA and t tests were used to determine the effect of genotype on behavioral preference. Open-field, elevated-plus-maze, and rotarod tests were performed as described previously (Parks et al., 1998).

Histological and Cell Biological Studies

In situ hybridization was performed using a fragment (nucleotides 1–1,260 from the start codon) of the *KIF13A* cDNA as described previously (Zhou et al., 2009). Brains were dissected and prepared for hematoxylin and eosin (H&E) staining as previously described (Takei et al., 2000). Samples were microphotographed using a microscope equipped with a digital camera (Leica Microsystems, Wetzler, Germany). Dissociated hippocampal neurons were prepared as described previously (Banker and Goslin, 1991). Hippocampal neurons were transfected by the Ca^{2+} phosphate method (Jiang and Chen, 2006). Fluorescent signals were observed using a LSM710 confocal microscope (Zeiss).

Antibodies

The anti-KIF13A and anti-5HT$_{1A}$R antibodies were raised in New Zealand white rabbits using custom antigen peptides as described previously (Niwa et al., 2008). Anti-GM130 antibody was purchased from BD Biosciences (San Jose, CA); anti-5HT$_{1A}$R antibody (1:500, catalog no. 85615), anti-5HT1BR antibody (1:300, catalog no. 13896), and anti-5HT2C receptor antibody (1:300, catalog no. 44640) were purchased from Abcam (Cambridge, MA); and anti-GluR3 antibody (1:300, catalog no. 3437) was purchased from Cell Signaling (Danvers, MA). These serotonin receptor antibodies were used in previous studies.

Binding Assays and RNA Interference

Immunoprecipitation, yeast two-hybrid, GST pull-down, and RNA interference (RNAi) assays were performed as described previously (Niwa et al., 2008).

ELISA of Secreted 5-HT

Determination of secreted 5-HT was performed using a 5-HT ELISA kit (Enzo Life Sciences, Farmingdale, NY) according to the manufacturer's instructions.

In Vitro Reconstitution Assay

An in vitro reconstitution assay was performed as described previously, with slight modifications (Nangaku et al., 1994). Total internal reflection fluorescence (TIRF) microscopy and fluorescence-labeled samples were used instead of differential interference contrast microscopy.

REFERENCES

Aiba, A., Chen, C., Herrup, K., Rosenmund, C., Stevens, C.F., and Tonegawa, S. (1994). Reduced hippocampal long-term potentiation and context-specific deficit in associative learning in mGluR1 mutant mice. Cell 79, 365–375.

Al Awabdh, S., Miserey-Lenkei, S., Bouceba, T., Masson, J., Kano, F., Marinach-Patrice, C., Hamon, M., Emerit, M.B., and Darmon, M. (2012). A new vesicular scaffolding complex mediates the G-protein-coupled 5-HT1A receptor targeting to neuronal dendrites. J. Neurosci. 32, 14227–14241.

Azmitia, E.C., Yu, I., Akbari, H.M., Kheck, N., Whitaker-Azmitia, P.M., and Marshak, D.R. (1992). Antipeptide antibodies against the 5-HT1A receptor. J. Chem. Neuroanat. 5, 289–298.

Banker, G., and Goslin, K. (1991). Culturing Nerve Cells (Cambridge, MA: MIT Press).

Cadogan, A.K., Kendall, D.A., and Marsden, C.A. (1994). Serotonin 5-HT1A receptor activation increases cyclic AMP formation in the rat hippocampus in vivo. J. Neurochem. 62, 1816–1821.

Carrel, D., Masson, J., Al Awabdh, S., Capra, C.B., Lenkei, Z., Hamon, M., Emerit, M.B., and Darmon, M. (2008). Targeting of the 5-HT1A serotonin receptor to neuronal dendrites is mediated by Yif1B. J. Neurosci. 28, 8063–8073.

Chen, A.C., Shirayama, Y., Shin, K.H., Neve, R.L., and Duman, R.S. (2001). Expression of the cAMP response element binding protein (CREB) in hippocampus produces an antidepressant effect. Biol. Psychiatry 49, 753–762.

Chow, A., Toomre, D., Garrett, W., and Mellman, I. (2002). Dendritic cell maturation triggers retrograde MHC class II transport from lysosomes to the plasma membrane. Nature 418, 988–994.

Chu, P.J., Rivera, J.F., and Arnold, D.B. (2006). A role for Kif17 in transport of Kv4.2. J. Biol. Chem. 281, 365–373.

Delevoye, C., Hurbain, I., Tenza, D., Sibarita, J.B., Uzan-Gafsou, S., Ohno, H., Geerts, W.J., Verkleij, A.J., Salamero, J., Marks, M.S., and Raposo, G. (2009). AP-1 and KIF13A coordinate endosomal sorting and positioning during melanosome biogenesis. J. Cell Biol. 187, 247–264.

Dotti, C.G., and Banker, G. (1991). Intracellular organization of hippocampal neurons during the development of neuronal polarity. J. Cell Sci. Suppl. 15, 75–84.

Fricker, A.D., Rios, C., Devi, L.A., and Gomes, I. (2005). Serotonin receptor activation leads to neurite outgrowth and neuronal survival. Brain Res. Mol. Brain Res. 138, 228–235.

Ghavami, A., Stark, K.L., Jareb, M., Ramboz, S., Ségu, L., and Hen, R. (1999). Differential addressing of 5-HT1A and 5-HT1B receptors in epithelial cells and neurons. J. Cell Sci. 112, 967–976.

Glater, E.E., Megeath, L.J., Stowers, R.S., and Schwarz, T.L. (2006). Axonal transport of mitochondria requires milton to recruit kinesin heavy chain and is light chain independent. J. Cell Biol. 173, 545–557.

Gordon, J.A., and Hen, R. (2004). The serotonergic system and anxiety. Neuromolecular Med. 5, 27–40.

Gross, C., Zhuang, X., Stark, K., Ramboz, S., Oosting, R., Kirby, L., Santarelli, L., Beck, S., and Hen, R. (2002). Serotonin1A receptor acts during development to establish normal anxiety-like behaviour in the adult. Nature 416, 396–400.

Guillaud, L., Setou, M., and Hirokawa, N. (2003). KIF17 dynamics and regulation of NR2B trafficking in hippocampal neurons. J. Neurosci. 23, 131–140.

Hall, D.H., and Hedgecock, E.M. (1991). Kinesin-related gene unc-104 is required for axonal transport of synaptic vesicles in C. elegans. Cell 65, 837–847.

Hamm, R.J., Pike, B.R., O'Dell, D.M., Lyeth, B.G., and Jenkins, L.W. (1994). The rotarod test: an evaluation of its effectiveness in assessing motor deficits following traumatic brain injury. J. Neurotrauma 11, 187–196.

Hedstrom, K.L., Ogawa, Y., and Rasband, M.N. (2008). AnkyrinG is required for maintenance of the axon initial segment and neuronal polarity. J. Cell Biol. 183, 635–640.

Heisler, L.K., Chu, H.M., Brennan, T.J., Danao, J.A., Bajwa, P., Parsons, L.H., and Tecott, L.H. (1998). Elevated anxiety and antidepressant-like responses in serotonin 5-HT1A receptor mutant mice. Proc. Natl. Acad. Sci. USA 95, 15049–15054.

Hendricks, T.J., Fyodorov, D.V., Wegman, L.J., Lelutiu, N.B., Pehek, E.A., Yamamoto, B., Silver, J., Weeber, E.J., Sweatt, J.D., and Deneris, E.S. (2003). Pet-1 ETS gene plays a critical role in 5-HT neuron development and is required for normal anxiety-like and aggressive behavior. Neuron 37, 233–247.

Hirokawa, N., Niwa, S., and Tanaka, Y. (2010). Molecular motors in neurons: transport mechanisms and roles in brain function, development, and disease. Neuron 68, 610–638.

Horiguchi, K., Hanada, T., Fukui, Y., and Chishti, A.H. (2006). Transport of PIP3 by GAKIN, a kinesin-3 family protein, regulates neuronal cell polarity. J. Cell Biol. 174, 425–436.

Jiang, M., and Chen, G. (2006). High Ca2+-phosphate transfection efficiency in low-density neuronal cultures. Nat. Protoc. 1, 695–700.

Kanai, Y., Dohmae, N., and Hirokawa, N. (2004). Kinesin transports RNA: isolation and characterization of an RNA-transporting granule. Neuron 43, 513–525.

Kobayashi, T., Storrie, B., Simons, K., and Dotti, C.G. (1992). A functional barrier to movement of lipids in polarized neurons. Nature 359, 647–650.

Kondo, M., Takei, Y., and Hirokawa, N. (2012). Motor protein KIF1A is essential for hippocampal synaptogenesis and learning enhancement in an enriched environment. Neuron 73, 743–757.

Li, Y., Erzurumlu, R.S., Chen, C., Jhaveri, S., and Tonegawa, S. (1994). Whisker-related neuronal patterns fail to develop in the trigeminal brainstem nuclei of NMDAR1 knockout mice. Cell 76, 427–437.

Nakada, C., Ritchie, K., Oba, Y., Nakamura, M., Hotta, Y., Iino, R., Kasai, R.S., Yamaguchi, K., Fujiwara, T., and Kusumi, A. (2003). Accumulation of anchored proteins forms membrane diffusion barriers during neuronal polarization. Nat. Cell Biol. 5, 626–632.

Nakagawa, T., Tanaka, Y., Matsuoka, E., Kondo, S., Okada, Y., Noda, Y., Kanai, Y., and Hirokawa, N. (1997). Identification and classification of 16

new kinesin superfamily (KIF) proteins in mouse genome. Proc. Natl. Acad. Sci. USA 94, 9654–9659.

Nakagawa, T., Setou, M., Seog, D.H., Ogasawara, K., Dohmae, N., Takio, K., and Hirokawa, N. (2000). A novel motor, KIF13A, transports mannose-6-phosphate receptor to plasma membrane through direct interaction with AP-1 complex. Cell 103, 569–581.

Nakata, T., Terada, S., and Hirokawa, N. (1998). Visualization of the dynamics of synaptic vesicle and plasma membrane proteins in living axons. J. Cell Biol. 140, 659–674.

Nangaku, M., Sato-Yoshitake, R., Okada, Y., Noda, Y., Takemura, R., Yamazaki, H., and Hirokawa, N. (1994). KIF1B, a novel microtubule plus end-directed monomeric motor protein for transport of mitochondria. Cell 79, 1209–1220.

Nicholls, J.G. (2001). From Neuron to Brain, Fourth Edition (Sunderland, MA: Sinauer Associates).

Niwa, S., Tanaka, Y., and Hirokawa, N. (2008). KIF1Bbeta- and KIF1A-mediated axonal transport of presynaptic regulator Rab3 occurs in a GTP-dependent manner through DENN/MADD. Nat. Cell Biol. 10, 1269–1279.

Park, S.K., Nguyen, M.D., Fischer, A., Luke, M.P., Affar, B., Dieffenbach, P.B., Tseng, H.C., Shi, Y., and Tsai, L.H. (2005). Par-4 links dopamine signaling and depression. Cell 122, 275–287.

Parks, C.L., Robinson, P.S., Sibille, E., Shenk, T., and Toth, M. (1998). Increased anxiety of mice lacking the serotonin1A receptor. Proc. Natl. Acad. Sci. USA 95, 10734–10739.

Ramboz, S., Oosting, R., Amara, D.A., Kung, H.F., Blier, P., Mendelsohn, M., Mann, J.J., Brunner, D., and Hen, R. (1998). Serotonin receptor 1A knockout: an animal model of anxiety-related disorder. Proc. Natl. Acad. Sci. USA 95, 14476–14481.

Raymond, J.R., Kim, J., Beach, R.E., and Tisher, C.C. (1993a). Immunohistochemical mapping of cellular and subcellular distribution of 5-HT1A receptors in rat and human kidneys. Am. J. Physiol. 264, F9–F19.

Raymond, J.R., Olsen, C.L., and Gettys, T.W. (1993b). Cell-specific physical and functional coupling of human 5-HT1A receptors to inhibitory G protein alpha-subunits and lack of coupling to Gs alpha. Biochemistry 32, 11064–11073.

Renner, U., Glebov, K., Lang, T., Papusheva, E., Balakrishnan, S., Keller, B., Richter, D.W., Jahn, R., and Ponimaskin, E. (2007). Localization of the mouse 5-hydroxytryptamine(1A) receptor in lipid microdomains depends on its palmitoylation and is involved in receptor-mediated signaling. Mol. Pharmacol. 72, 502–513.

Roth, B.L. (2006). The Serotonin Receptors: From Molecular Pharmacology to Human Therapeutics (Totowa, NJ: Humana Press).

Roth, B.L., and Xia, Z. (2004). Molecular and cellular mechanisms for the polarized sorting of serotonin receptors: relevance for genesis and treatment of psychosis. Crit. Rev. Neurobiol. 16, 229–236.

Sagona, A.P., Nezis, I.P., Pedersen, N.M., Liestøl, K., Poulton, J., Rusten, T.E., Skotheim, R.I., Raiborg, C., and Stenmark, H. (2010). PtdIns(3)P controls cytokinesis through KIF13A-mediated recruitment of FYVE-CENT to the midbody. Nat. Cell Biol. 12, 362–371.

Sakai, K., and Miyazaki, J. (1997). A transgenic mouse line that retains Cre recombinase in mature oocytes irrespective of the cre transgene transmission. Biochem. Biophys. Res. Commun. 237, 318–324.

Schmidt, M.R., Maritzen, T., Kukhtina, V., Higman, V.A., Doglio, L., Barak, N.N., Strauss, H., Oschkinat, H., Dotti, C.G., and Haucke, V. (2009). Regulation of endosomal membrane traffic by a Gadkin/AP-1/kinesin KIF5 complex. Proc. Natl. Acad. Sci. USA 106, 15344–15349.

Setou, M., Nakagawa, T., Seog, D.H., and Hirokawa, N. (2000). Kinesin superfamily motor protein KIF17 and mLin-10 in NMDA receptor-containing vesicle transport. Science 288, 1796–1802.

Snyder, S.H. (2009). Neurotransmitters, receptors, and second messengers galore in 40 years. J. Neurosci. 29, 12717–12721.

Stowers, R.S., Megeath, L.J., Górska-Andrzejak, J., Meinertzhagen, I.A., and Schwarz, T.L. (2002). Axonal transport of mitochondria to synapses depends on milton, a novel Drosophila protein. Neuron 36, 1063–1077.

Takei, Y., Teng, J., Harada, A., and Hirokawa, N. (2000). Defects in axonal elongation and neuronal migration in mice with disrupted tau and map1b genes. J. Cell Biol. 150, 989–1000.

Tsien, J.Z., Huerta, P.T., and Tonegawa, S. (1996). The essential role of hippocampal CA1 NMDA receptor-dependent synaptic plasticity in spatial memory. Cell 87, 1327–1338.

Vale, R.D. (2003). The molecular motor toolbox for intracellular transport. Cell 112, 467–480.

Verhey, K.J., and Hammond, J.W. (2009). Traffic control: regulation of kinesin motors. Nat. Rev. Mol. Cell Biol. 10, 765–777.

Wang, X., and Schwarz, T.L. (2009). The mechanism of Ca2+ -dependent regulation of kinesin-mediated mitochondrial motility. Cell 136, 163–174.

Weigert, R., Yeung, A.C., Li, J., and Donaldson, J.G. (2004). Rab22a regulates the recycling of membrane proteins internalized independently of clathrin. Mol. Biol. Cell 15, 3758–3770.

Yin, X., Takei, Y., Kido, M.A., and Hirokawa, N. (2011). Molecular motor KIF17 is fundamental for memory and learning via differential support of synaptic NR2A/2B levels. Neuron 70, 310–325.

Zhou, F.C., Patel, T.D., Swartz, D., Xu, Y., and Kelley, M.R. (1999). Production and characterization of an anti-serotonin 1A receptor antibody which detects functional 5-HT1A binding sites. Brain Res. Mol. Brain Res. 69, 186–201.

Zhou, R., Niwa, S., Homma, N., Takei, Y., and Hirokawa, N. (2009). KIF26A is an unconventional kinesin and regulates GDNF-Ret signaling in enteric neuronal development. Cell 139, 802–813.